JACS
JOURNAL OF THE AMERICAN CHEMICAL SOCIETY
Communication
pubs.acs.org/JACS

# Shape-Dependent Hydrogen-Storage Properties in Pd Nanocrystals: Which Does Hydrogen Prefer, Octahedron (111) or Cube (100)?

Guangqin Li,[†] Hirokazu Kobayashi,*[,†,‡] Shun Dekura,[†] Ryuichi Ikeda,[†,‡] Yoshiki Kubota,[§] Kenichi Kato,[∥,⊥] Masaki Takata,[∥,⊥] Tomokazu Yamamoto,[‡,#] Syo Matsumura,[‡,#,○,▽] and Hiroshi Kitagawa*[,†,‡,▽,◆]

[†]Division of Chemistry, Graduate School of Science, Kyoto University, Kitashirakawa-Oiwakecho, Sakyo-ku, Kyoto 606-8502, Japan
[‡]JST CREST, Goban-cho 7, Chiyoda-ku, Tokyo 102-0075, Japan
[§]Department of Physical Science, Graduate School of Science, Osaka Prefecture University, Sakai, Osaka 599-8531, Japan
[∥]RIKEN SPring-8 Center, 1-1-1 Kouto, Sayo-cho, Sayo-gun, Hyogo 679-5148, Japan
[⊥]Japan Synchrotron Radiation Research Institute, 1-1-1 Kouto, Sayo-cho, Sayo-gun, Hyogo 679-5198, Japan
[#]Research Laboratory of High-Voltage Electron Microscope, Kyushu University, Motooka 744, Nishi-ku, Fukuoka 819-0395, Japan
[○]Department of Applied Quantum Physics and Nuclear Engineering, Kyushu University, Motooka 744, Nishi-ku, Fukuoka 819-0395, Japan
[▽]INAMORI Frontier Research Center, Kyushu University, Motooka 744, Nishi-ku, Fukuoka 819-0395, Japan
[◆]Institute for Integrated Cell-Material Sciences (iCeMS), Kyoto University, Yoshida, Sakyo-ku, Kyoto 606-8501, Japan

Supporting Information

**ABSTRACT:** Pd octahedrons and cubes enclosed by {111} and {100} facets, respectively, have been synthesized for investigation of the shape effect on hydrogen-absorption properties. Hydrogen-storage properties were investigated using in situ powder X-ray diffraction, in situ solid-state $^2$H NMR and hydrogen pressure−composition isotherm measurements. With these measurements, it was found that the exposed facets do not affect hydrogen-storage capacity; however, they significantly affect the absorption speed, with octahedral nanocrystals showing the faster response. The heat of adsorption of hydrogen and the hydrogen diffusion pathway were suggested to be dominant factors for hydrogen-absorption speed. Furthermore, in situ solid-state $^2$H NMR detected for the first time the state of $^2$H in a solid-solution (Pd + H) phase of Pd nanocrystals at rt.

The hydride of Pd has been intensively investigated in various fields of fundamental science and technology for developing hydrogen storage, purification filters, isotope separation, and electrodes for metal hydride batteries.[1] Many investigations into hydrogen storage using bulk Pd or Pd-based alloys have been carried out over the past half-century.[1] Recently, metal nanoparticles have attracted much attention, not only as electronic, magnetic, optical, and catalytic materials but also as a new type of hydrogen-storage metal.[2] In particular, Pd nanoparticles have been studied as a model for the clarification of hydrogen-storage properties of metal nanoparticles.[2a−f] The hydrogen concentration and equilibrium pressure for the formation of Pd hydride were reported to decrease with a decrease in the particle size.[2a] In addition, it was shown that compared with bulk Pd, hydrogen atoms are strongly trapped inside Pd nanoparticles because of the formation of stable Pd−H bonds.[2b]

Very recently, in addition to size, the shape of metal nanoparticles has been also critical to modern materials chemistry because the intrinsic properties are strongly correlated with their morphologies.[3] Pd nanoparticles exposed with {111} facets are active for CO oxidative coupling to dimethyl oxalate, whereas Pd nanoparticles exposed with {100} facets are inactive for this reaction.[3a] Pd nanoparticles with {100} facets exhibited higher acetylene hydrogenation activity and ethylene selectivity than the particles with {111} facets.[3b] Some recent studies have been carried out to investigate the catalytic behaviors of different morphologies, but there are no reports on how the shape of the nanocrystals may affect the hydrogen storage properties of Pd. Research into the interaction between metals and hydrogen is very important for the development of potential applications, such as effective catalysts for hydrogenation or advanced materials for hydrogen storage and purification. Here, we report for the first time the hydrogen-storage properties of shape-controlled Pd nanocrystals. The hydrogen-storage properties were investigated using hydrogen pressure−composition (PC) isotherms, *in situ* powder X-ray diffraction (XRD), and *in situ* solid-state $^2$H NMR measurements.

We chose Pd octahedrons and cubes to investigate the shape effect on hydrogen-absorption properties. Pd octahedrons and cubes enclosed by {111} and {100} facets, respectively, were prepared in a water-based system, as reported previously.[4] Figure 1a and 1b show transmission electron microscopy (TEM) images of the obtained Pd octahedrons and cubes, respectively. From the TEM images, mean diameters were

**Received:** May 19, 2014
**Published:** July 14, 2014

   dx.doi.org/10.1021/ja504699u | J. Am. Chem. Soc. 2014, 136, 10222−10225

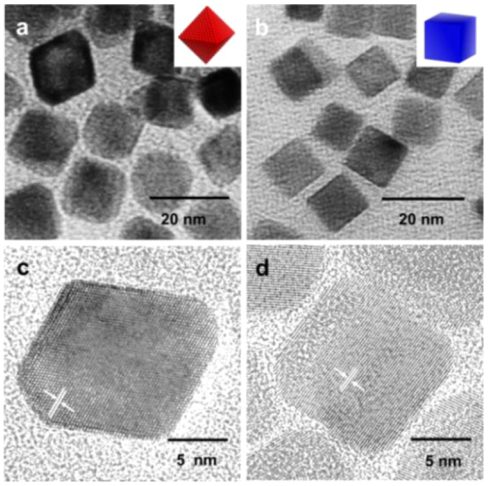


**Figure 1.** TEM and HRTEM images of Pd octahedrons (a, c) and Pd cubes (b, d).

estimated to be 11.6 nm for the octahedrons and 10.5 nm for the cubes. The surface atomic ratios of the octahedrons and the cubes were 25% and 21%, respectively.

From high-resolution (HR) TEM images (Figure 1c and 1d), it was shown that both the octahedrons and the cubes have good crystalline structures and the distances of the lattice fringes were 2.25 Å for the octahedrons and 1.97 Å for the cubes, corresponding to the lattice *d*-spacings of {111} and {100} of face-centered-cubic (fcc) Pd, respectively. From the powder X-ray diffraction (XRD) patterns (Figure S1), the crystal sizes of Pd octahedrons and cubes were estimated by Le Bail fitting of the XRD patterns to be 12.1 and 10.6 nm, respectively, which is consistent with the TEM results (Figures 1a and 1b).

It is known that the hydrogen-absorption/desorption process of Pd involves a first-order transition, and the phase transition from the solid solution ($\alpha$-phase) to the hydride ($\beta$-phase) results in an expansion in the Pd lattice.[1,2a,b] We elucidated the structural change during the hydrogen absorption process under controlled hydrogen pressure using *in situ* XRD measurements at the BL02B2 beamline at the Super Photon Ring (SPring-8)[5] (Figures S2 and S3). The XRD patterns were recorded at every 10 min for each pressure. For both the octahedrons and the cubes during hydrogen absorption, the diffraction peaks from the fcc hydride $\beta$-phase lattice began to appear at 24.7° ($2\theta$), in addition to the unchanged diffraction from the $\alpha$-phase solid solution Pd lattice at 25.7° ($2\theta$). The ratios of $\beta$-phase in Pd octahedrons and cubes were determined by Rietveld refinement of the powder XRD patterns at 101.3 kPa of hydrogen pressure. The $\beta$-phase ratios for the octahedrons and cubes were 72% and 58%, respectively, after equivalent equilibration times at 101.3 kPa (Figure S4). The relatively large ratio of the $\beta$-phase for octahedrons suggests that the octahedrons absorb hydrogen faster than the cubes.

We investigated the hydrogen-absorption speed of the octahedrons and cubes by the time dependence of XRD measurements recorded every 5 min under 101.3 kPa of constant $H_2$ pressure (Figures 2a, 2b, S5, and S6). For the octahedrons, the diffraction peaks from the $\beta$-phase lattice increased over time, while the diffraction peaks from the $\alpha$-phase decreased. Within 20 min, the $\beta$-phase became the dominant component (Figure 2a). On the other hand, for the cubes, the components of the $\alpha$- and $\beta$-phase were almost the

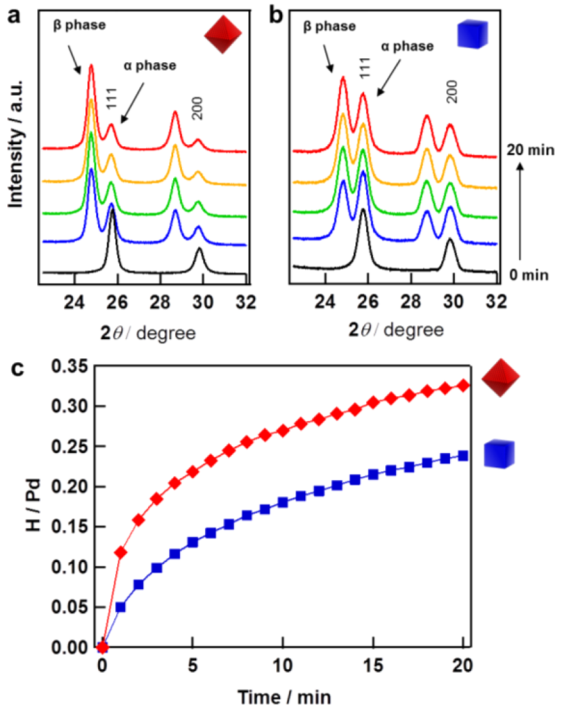


**Figure 2.** Time dependency of XRD patterns of (a) Pd octahedrons and (b) cubes under 101.3 kPa of hydrogen pressure. (c) Isothermal hydrogenation profiles of Pd octahedrons (red) and cubes (blue) at 303 K after introducing hydrogen pressure of 101.3 kPa.

same ratio over the same time period. The ratios of the $\beta$-phase in Pd octahedrons and cubes were estimated using the Rietveld refinement of the XRD patterns. As shown in Figure S7, it can be observed that the $\beta$-phase ratio in the octahedrons was 77% within 20 min, but only 56% for the cubes after the same period of time. This result strongly supports the conclusion that octahedrons have a faster response for hydrogen storage compared with cubes.

To obtain direct evidence of the hydrogen storage speed of the Pd octahedrons and cubes, the kinetics of the hydrogenation were investigated by isothermal hydrogenation profiles at 303 K, after introducing a hydrogen pressure of 101.3 kPa, as shown in Figure 2c. Pd octahedrons took up 0.27 H/Pd within 10 min, while the cubes absorbed 0.18 H/Pd.[6] These results indicate that the octahedrons absorb hydrogen 1.5 times as fast as Pd cubes within the first 10 min. After 150 min, the octahedrons and the cubes had the same amount of hydrogen (Figure S8).

The hydrogen-absorption process of bulk Pd is divided mainly into three steps (Figure 3).[1] First, hydrogen molecules dissociate into atoms on the surface of Pd (I → II), and then the atoms penetrate the subsurface (II → III). Finally, the atoms diffuse into the octahedral interstitial sites in the Pd lattice to form the hydride (Pd−H) (III → IV). The dissociation of hydrogen molecules into atoms (I → II) is reported to be the rate-limiting step below 200 K, but it is negligible at 303 K.[1,7] In this study, the diffusion of the atoms from surface to subsurface (II → III) is considered to be the dominant factor for hydrogen-absorption speed. The initial heat of adsorption of hydrogen ($E_H$) for the Pd {100} substrate is claimed to be larger than that for the Pd {111} substrate; i.e., the atoms on Pd {100} are more stable than those on Pd {111}.[7] In addition, for Pd {111}, the hydrogen atoms can


dx.doi.org/10.1021/ja504699u | J. Am. Chem. Soc. 2014, 136, 10222−10225

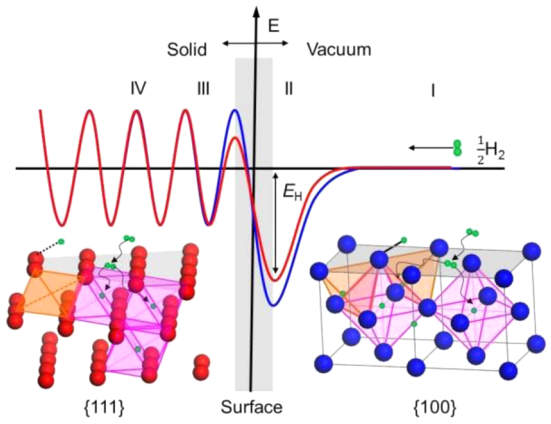


**Figure 3.** Schematic potential energy diagrams of the Pd octahedrons {111}/H (red) and the cubes {100}/H (blue) systems.

directly diffuse into the octahedral sites.[8] On the other hand, for Pd {100}, hydrogen atoms first go through tetrahedral sites and then diffuse into octahedral sites.[9] The relatively large $E_H$ and the pathway to tetrahedral sites for Pd {100} having a high potential barrier result in the slower hydrogen-absorption speed of Pd {100} compared with Pd {111}. The new finding, in this report, provides a strategy for the development of efficient hydrogen-storage materials with a high hydrogen-absorption speed.

To investigate the hydrogen-absorption capacity of Pd octahedrons and cubes, the PC isotherms were measured at 303 K (Figure S9). For both morphologies, the hydrogen concentration increased with hydrogen pressure, and the total amount of hydrogen absorption at 101.3 kPa was 0.48 H/Pd for the octahedrons, almost the same capacity as 0.50 H/Pd for the cubes.[6] It should be noted that the pressure of the plateau-like region in the octahedrons, where solid solution (Pd + H, $\alpha$) and hydride (Pd−H, $\beta$) phases coexist, became more obvious than that in cubes. In addition, the PC isotherm of the octahedrons returns to the starting point on desorption, unlike the case with cubes. The obvious plateau region and the recovery of the PC isotherms of the octahedrons support that octahedrons have a faster response for hydrogen storage compared to the cubes.

We performed *in situ* solid-state $^2$H NMR measurements under various deuterium gas ($^2H_2$) pressures to investigate the states of $^2$H in the nanocrystals (Figure 4a and 4b). For the octahedrons during the absorption process (Figure 4a), no signals were observed up to 5 kPa of $^2H_2$ gas because of the low $^2H_2$ concentration (Figure S10). At 10 kPa of $^2H_2$ gas, a broad absorption line appeared at 10 ppm and a signal from $^2H_2$ gas at 3.2 ppm. The broad component is attributed to deuterium atoms ($^2$H) with restricted motion within the Pd lattice as a Pd−$^2$H hydride ($\beta$-phase).[2b,c] The broad component shifted gradually to lower magnetic field, and the chemical shift reached 30.4 ppm at 101.3 kPa. In the desorption process, the hydride component was shifted to higher magnetic field with decreasing $^2H_2$ gas pressure. The hydride component of the cubes exhibited similar behavior as the octahedrons with the formation of a $\beta$-phase (Figure 4b). The chemical shift values of the hydride component observed for the octahedrons and the cubes are summarized in Figure S11. It can be seen that the shift value increases with $^2H_2$ gas pressure for both the octahedrons and the cubes, which indicates that the *d* band in Pd hydride is almost filled, so the *d* spin correlation is

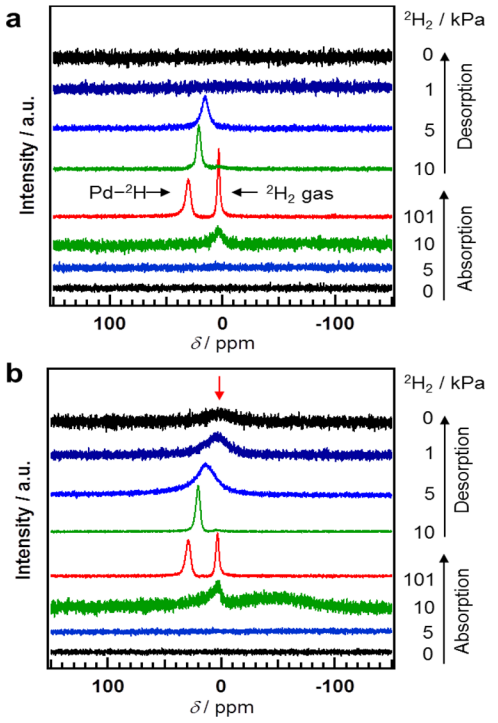


**Figure 4.** *In situ* solid-state $^2$H NMR spectra of (a) Pd octahedrons and (b) cubes under the absorption/desorption process at 303 K.

weakened, and the Knight shift arising from *s* conduction electrons is the dominant factor.[10] It should be noted that the chemical shift showed a hysteresis upon the absorption/desorption process, which is analogous to the hysteresis observed in the PC isotherms.

Interestingly, at 0 kPa in the desorption process, the broad signal of deuterium atoms inside the Pd lattice disappeared for the octahedrons (Figure 4a), while the signal was still observed at 2.3 ppm for the cubes (Figure 4b). This result suggests that hydrogen atoms are more strongly trapped and stabilized in the lattice of the cubes compared with the octahedrons, which results in the incomplete recovery of the PC isotherm observed at 303 K shown in Figure S9.

At 10 kPa in the absorption process, a much broader signal in the cubes was observed at an upfield shift (ca. −50 ppm) in addition to the signal of $^2$H in Pd hydride shown in Figure 4b. To clarify the origin of this broad upfield signal, we performed *in situ* solid-state $^2$H NMR measurements in the pressure range between 5 and 20 kPa, shown in Figure 5. At 8 kPa, the upfield signal was clearly observed, and the signal intensity decreased with increasing $^2H_2$ pressure and disappeared at 20 kPa, while the downfield $\beta$-phase component of Pd−$^2$H hydride increased. Taking into consideration that these pressures correspond to the plateau-like region, where solid solution (Pd + H, $\alpha$) and hydride (Pd−H, $\beta$) phases coexist in the PC isotherm, the upfield signal is attributed to deuterium atoms ($^2$H) within the Pd lattice as the $\alpha$-phase. This upfield shift observed in the Pd cubes can be explained by the $^2$H *s* spin's being polarized by the *d* spin paramagnetism of the Pd. That is, in the $\alpha$-phase with a low hydrogen concentration, the density of states at the Fermi level of the Pd is mainly composed of a 4d band; as a result, the spin correlation between the $^2$H *s* spin and the Pd *d* spin is the dominant factor to causing the upfield shift. On the other hand, due to the obvious plateau region and high hydrogen concentration (ca. 0.4 H/Pd at 10 kPa) in the octahedrons,


dx.doi.org/10.1021/ja504699u | J. Am. Chem. Soc. 2014, 136, 10222−10225

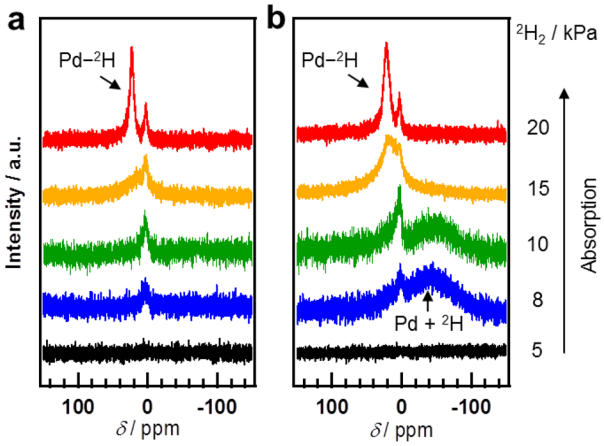


**Figure 5.** *In situ* solid-state $^2$H NMR spectra of (a) Pd octahedrons and (b) cubes under absorption from 5 to 20 kPa.

compared to those in the cubes (ca. 0.3 H/Pd at 10 kPa) (Figure S9), the $\beta$-phase is considered to be the main component, resulting in the unobservable NMR signal originating from the $\alpha$-phase for the octahedrons.

Pd is one of the best known hydrogen-storage metals, and its hydrogen-storage properties have been extensively investigated for many years.[1] While research on the hydride (Pd–H, $\beta$) phase has been extensive, there is little experimental observation on the state of hydrogen atoms dissolved in the Pd lattice (Pd + H, $\alpha$) because of the extremely low hydrogen concentration. Solid-state NMR is very sensitive and a powerful probe to evaluate hydrogen atoms inside metals. This is the first direct observation of a $^2$H NMR signal in the $\alpha$-phase of Pd nanocrystals at rt.

In summary, we have synthesized and characterized Pd octahedrons and cubes enclosed by {111} and {100} facets for the first investigation into the hydrogen-absorption properties of shape-controlled Pd nanocrystals. The octahedrons can absorb the same amount of hydrogen as the cubes, but the kinetics of absorption change with shape. The octahedrons with {111} facets exhibited rapid kinetics for hydrogen storage, compared with the cubes with {100} facets, originating from the differences in the heat of adsorption of hydrogen and the hydrogen diffusion pathway. In addition, for the first time, we observed the state of $^2$H in the solid-solution phase by in situ solid-state $^2$H NMR measurements. These new findings provide clues not only for the development of effective hydrogen-storage materials but also for clarification of the catalysis mechanism associated with hydrogen and Pd nanocrystals.

## ■ ASSOCIATED CONTENT

### Ⓢ Supporting Information

*In situ* XRD patterns, isothermal hydrogenation profiles, PC isotherms, and solid-state $^2$H NMR spectra. This material is available free of charge via the Internet at http://pubs.acs.org.

## ■ AUTHOR INFORMATION

### Corresponding Authors

hkobayashi@kuchem.kyoto-u.ac.jp
kitagawa@kuchem.kyoto-u.ac.jp

### Notes

The authors declare no competing financial interest.

## ■ ACKNOWLEDGMENTS

Synchrotron XRD measurements were supported by the Japan Synchrotron Radiation Research Institute (JASRI) (Proposal No. 2012B1516). HRTEM images were performed partly as a research program (A-13-KU-0100) of the Nanotechnology Platform project conducted by MEXT. G.L. is grateful for a PhD fellowship donated by the China Scholarship Council (CSC).

## ■ REFERENCES

(1) (a) Lewis, F. A. *The Palladium Hydrogen System*; Academic Press: London, 1967. (b) Alefeld, G., Völkl, J., Eds. *Hydrogen in Metals II*; Springer: Berlin, Heidelberg, 1978.

(2) (a) Yamauchi, M.; Ikeda, R.; Kitagawa, H.; Takata, M. *J. Phys. Chem. C* **2008**, *112*, 3294. (b) Kobayashi, H.; Yamauchi, M.; Kitagawa, H.; Kubota, Y.; Kato, K.; Takata, M. *J. Am. Chem. Soc.* **2008**, *130*, 1828. (c) Yamauchi, M.; Kobayashi, H.; Kitagawa, H. *ChemPhysChem* **2009**, *10*, 2566. (d) Pundt, A.; Sachs, C.; Winter, M.; Reetz, M. T.; Fritsch, D.; Kirchheim, R. *J. Alloys Compd.* **1999**, *293–295*, 480. (e) Sachs, C.; Pundt, A.; Kirchheim, R. *Phys. Rev. B* **2001**, *64*, 075408. (f) Yamauchi, M.; Kitagawa, H. *Synth. Met.* **2005**, *153*, 353. (g) Kobayashi, H.; Morita, H.; Yamauchi, M.; Ikeda, R.; Kitagawa, H.; Kubota, Y.; Kato, K.; Takata, M. *J. Am. Chem. Soc.* **2012**, *134*, 12390. (h) Kobayashi, H.; Yamauchi, M.; Kitagawa, H.; Kubota, Y.; Kato, K.; Takata, M. *J. Am. Chem. Soc.* **2008**, *130*, 1818. (i) Kobayashi, H.; Morita, H.; Yamauchi, M.; Ikeda, R.; Kitagawa, H.; Kubota, Y.; Kato, K.; Takata, M. *J. Am. Chem. Soc.* **2011**, *133*, 11034. (j) Kobayashi, H.; Yamauchi, M.; Kitagawa, H. *J. Am. Chem. Soc.* **2012**, *134*, 6893. (k) Kobayashi, H.; Yamauchi, M.; Kitagawa, H.; Kubota, Y.; Kato, K.; Takata, M. *J. Am. Chem. Soc.* **2010**, *132*, 5576. (l) Kobayashi, H.; Yamauchi, M.; Ikeda, R.; Kitagawa, H. *Chem. Commun.* **2009**, 4806.

(3) (a) Xu, Z. N.; Sun, J.; Lin, C. S.; Jiang, X. M.; Chen, Q. S.; Peng, S. Y.; Wang, M. S.; Guo, G. C. *ACS Catal.* **2013**, *3*, 118. (b) Kim, S. K.; Kim, C.; Lee, J. H.; Kim, J.; Lee, H.; Moon, S. H. *J. Catal.* **2013**, *306*, 146. (c) Crespo, Q. M.; Yarulin, A.; Jin, M.; Xia, Y.; Minsker, K. L. *J. Am. Chem. Soc.* **2011**, *133*, 12787. (d) Xia, Y. N.; Xiong, Y.; Lim, B.; Skrabalak, S. E. *Angew. Chem., Int. Ed.* **2009**, *48*, 60. (e) Puntes, V. F.; Krishnan, K. M.; Alivisatos, A. P. *Science* **2001**, *291*, 2115. (f) Tian, N.; Zhou, Z. Y.; Sun, S. G.; Ding, Y.; Wang, Z. L. *Science* **2007**, *316*, 732. (g) Sun, Y.; Xia, Y. *Science* **2002**, *298*, 2176. (h) Lee, H.; Habas, S. E.; Kweskin, S.; Butcher, D.; Somorjai, G. A.; Yang, P. *Angew. Chem., Int. Ed.* **2006**, *118*, 7988. (i) Tao, A. R.; Habas, S.; Yang, P. *Small* **2008**, *4*, 310. (j) Habas, S. E.; Lee, H.; Radmilovic, V.; Somorjai, G. A.; Yang, P. *Nat. Mater.* **2007**, *6*, 602. (k) Gu, J.; Zhang, Y. W.; Tao, F. *Chem. Soc. Rev.* **2012**, *41*, 8050.

(4) Lim, B.; Jiang, M.; Tao, J.; Camargo, P. H. C.; Zhu, Y.; Xia, Y. *Adv. Funct. Mater.* **2009**, *19*, 189.

(5) Nishibori, E.; et al. *Nucl. Instrum. Methods Phys. Res., Sect. A* **2001**, *467–468*, 1045.

(6) Li, G.; Kobayashi, H.; Taylor, J. M.; Ikeda, R.; Kubota, Y.; Kato, K.; Takata, M.; Yamamoto, T.; Toh, S.; Matsumura, S.; Kitagawa, H. *Nat. Mater.* **2014**, DOI: 10.1038/nmat4030.

(7) Christmann, K. *Surf. Sci. Rep.* **1988**, *9*, 1.

(8) Ozawa, N.; Roman, T. A.; Nakanishi, H.; Kasai, H.; Arboleda, N. B., Jr.; Diño, W. A. *J. Appl. Phys.* **2007**, *101*, 123530.

(9) Okuyama, H.; Siga, W.; Takagi, N.; Nishijima, M.; Aruga, T. *Surf. Sci.* **1998**, *401*, 344–354.

(10) Barabino, D. J.; Dybowski, C. *Solid State Nucl. Magn. Reson.* **1992**, *1*, 5.